Eye (2009) 23, 652–660

www.nature.com/eye

CLINICAL STUDY

Telemedical diagnosis of anterior segment eye diseases: validation of digital slit-lamp still images

S Kumar[1], K Yogesan[1] and IJ Constable[2]

Abstract

Purpose **This study compared digital images from a portable slit-lamp camera with 35 mm slit-lamp photographs and traditional ophthalmic assessments in anterior segment disorder's detection.**

Methods **A total of 196 patients (392 eyes) were recruited from an anterior segment ophthalmology clinic. Each patient underwent an examination by an anterior segment ophthalmologist. Two to three standardized views of 640 × 480 pixels digital images (portable digital slit-lamp camera) and 35 mm photographic slides (Zeiss slit-lamp camera) were taken after the examination. The same ophthalmologist reviewed these images in a masked fashion. Two other masked graders also assessed the digital images. The presence or absence of 33 specific findings was noted at each examination.**

Results **Digital images showed moderate to excellent agreement to clinical findings (κ 0.45–0.82) in areas other than lid pathologies. Lens findings from digital images had moderate to good agreement with the clinical gold standard (unweighted κ 0.43–0.65, sensitivity 59–77%, specificity 86–94%). Gross cornea signs were well detected with digital images, (κ 0.72–0.85, sensitivity 67–100%, specificity 98–99). More subtle corneal, conjunctival and lid abnormalities were not identified well. The statistical figures were very similar to the above-mentioned figures when the 35-mm film results were compared to clinical diagnoses. The two image formats showed better agreement when compared to each other than when either is compared with clinical findings.**

Conclusion **Diagnoses using digital slit-lamp images were comparable to diagnosis using 35 mm photographic slides for some anterior segment abnormalities.**

Eye (2009) **23,** 652–660; doi:10.1038/eye.2008.11; published online 15 February 2008

Keywords: telemedicine; anterior segment eye disease; stored–forward; digital images

[1]Centre of Excellence in e-Medicine, University of Western Australia, Perth, Australia

[2]Lions Eye Institute, University of Western Australia, Perth, Australia

Correspondence: S Kumar, Centre of Excellence in e-Medicine Lions Eye Institute, University of Western Australia, 2 Verdun Street, Nedlands 6009, WA Australia.
Tel: +618 9381 0760;
Fax: +618 9381 0857.
E-mail: sajeesh@cyllene.uwa.edu.au

Received: 26 October 2007
Accepted in revised form: 14 January 2008
Published online: 15 February 2008

Introduction

Telemedicine has already become a common tool in image-based medical specialty such as ophthalmology.[1] This new method of service delivery offers a number of substantial advantages over conventional face-to-face consultations. This includes cost effectiveness,[2,3] improved service accessibility in remote areas,[4,5] and local health-care workers gaining more experience in ophthalmology through participation in telemedical consultations.[1,4,6]

There are several major components in a teleophthalmology system. These consist of image capture, digitisation, transmission, storage, interpretation, and finally a reply. Image capture is the beginning and perhaps the most vital part of the system. Poor quality images may lead to poor diagnosis. Image acquisition is particularly a problem in ophthalmology as the eye can only be examined thoroughly with expensive specialised optical instruments. For teleophthalmology, these instruments need to be modified for high-resolution digital capture, which further adds to the cost and complexity. On the other hand, these instruments need to be more affordable, portable, and less complex to widen the service access.[1]

The standard slit-lamp biomicroscope is the benchmark device for anterior segment ocular

examination. However, the complexity of the instrument together with the cost prohibits widespread use of it in remote communities. A portable and simplified instrument would be more suitable for the health-care workers in distant locations. A portable slit-lamp video camera has been developed at the Lions Eye Institute (LEI) in Perth, Western Australia (Figure 1). This hand-held instrument has a fixed width slit beam with two selectable alignments. A third 'red reflex' coaxial illumination is also selectable. Only four switches and one trigger are needed to control this digital slit-lamp camera. The switches adjust the intensity of the background illumination intensity, background illumination colour (blue or white), slit beam intensity, and the direction of the slit beam. The trigger activates image capture. There is a liquid crystal display panel on the unit to aid focusing. A frame grabber attached to a personal computer digitises the video images. The image resolution of the digital image is 640×480 pixels. A health-care worker with little background computer knowledge can be trained to use this camera to capture the standard images for this study in few hours.

Most research in the image capture component of teleophthalmology to date has been aimed at retinal pathologies. Although most of the published works have been descriptive in nature, there have been some comparative trials that compared images from video fundus cameras to 35 mm film in detection of diabetic retinopathy.[7–10] The results so far have been encouraging. Relatively little work has been done on anterior segment telemedical examinations. A feasibility study on ocular surface assessment using telemedical equipment was performed by Shimmura *et al*.[11] Threlkeld *et al*[12] examined the accuracy of telemedical anterior segment ocular examination. The use of a video slit-lamp in examination of postoperative cataract and glaucoma patients was investigated by Murdoch *et al*.[13] Schiffman *et al*[14] has described several years of experience using a teleophthalmology system with several different peripherals including video slit lamps. All these investigators used a combination of a standard slit-lamp biomicroscope and a CCD video camera attachment. Also, in most of these studies the video slit lamps were operating in a real-time mode.

Figure 1 Image of the hand held, portable digital slit-lamp (PSL) video camera developed at the Lions Eye Institute (LEI) in Perth, Western Australia. This hand held instrument has a fixed width slit beam with two selectable alignments. A third 'red reflex' coaxial illumination is also selectable.

There are two general system architectures in telemedicine. In a real-time or teleconferencing consultation, the local operator, the patient, and the remote specialist are all present and communicating. Video-conferencing equipment is one of the most common forms of real-time telemedicine. While in a store and forward system, digital images, video, audio, and clinical data are captured and 'stored' on the client computer; then at a convenient time, transmitted securely ('forwarded') to a clinic at another location where they are studied by relevant specialists. The opinion of the specialist is then transmitted back.

To the best of our knowledge, there has been no comparison study of a store and forward still image system against traditional method of service delivery in anterior segment ophthalmology. There has also been no formal comparison of digital anterior segment ophthalmic images against 35 mm slides. Using traditional examination and photographic methods as a comparison, this study aimed to investigate the accuracy of this new dedicated telemedicine camera in identifying and grading anterior segment eye diseases. Although the images were not transmitted electronically using telecommunication technology between computers, the design of this study simulated a store and forward telemedicine environment.

Methods

Patients attending the clinic of an anterior segment ophthalmologist at the Lions Eye Institute were recruited into this trial. The Patients were not selected on the basis of presence or absence of pathology. Because of the technical difficulties with the equipment, only 343 eyes had digital images taken and only 338 eyes had 35 mm slides taken.

Each patient was examined by an experienced anterior segment consultant ophthalmologist using a standard slit-lamp biomicroscope (Haag Streit BQ900, Bern, Switzerland). The presence or absence of 33 specific

findings were noted on a standardised scoring sheet (Table 1). Lens opacities were graded as 0, 1+, 2+, 3+, and 4+. A health worker with little experience in ophthalmology imaged the subject's eyes with the Zeiss (Carl Zeiss Jena GmbH) 40SL/P slit-lamp camera (ZSL) and the LEI portable slit-lamp camera (PSL) before or after the examination. Two standardised views were taken with the ZSL. A third retroillumination view was taken, if the patient had pupil dilation. Figure 2 summarises the instrument setup for each of these views. 30–40 s of video image were then captured from each eye with the PSL. Two frames (three in dilated patients) with the same standardised attributes were extracted from these video clips. The digital images are then saved and transferred to other computers through a CD-ROM.

Table 1 List of anterior segment abnormalities detected in this study

Ocular structure	*Abnormality*	*Ocular structure*	*Abnormality*
Cornea	Ulcer	Conjunctiva	Injection
	Abrasion		Pinguecula
	Oedema		Pterygium
	Vascularisation		Haemorrhage
	Epitheliopathy		Conjunctivitis
	Keratic precipitate	Eyelid	Entropion
	Scar		Ectropion
	Bullae		Trichiasis
	Lipid deposit		Papilloma
	Haze		Blepharitis
	Lasik flap	Iris	Iridectomy
	Graft		Irregular pupil
	Contact lens		Naevus
	Opacification	Lens	Nuclear sclerosis
Anterior chamber	Cells		Cortical opacity
	Flare		Post subcapsular opacity
			Intraocular lens

The same ophthalmologist assessed the still images captured from the two cameras in a masked fashion. The digital images were assessed several weeks after the initial clinic visit. One month after the digital image assessment sessions, 35 mm slides were presented. The assessor noted the findings using the same scoring sheet as that used in the clinical assessment stage. To give a measure of inter-reader agreement, two other ophthalmologists graded the digital images from the first 100 patients.

Steps were taken to match the image attributes between the two image formats. First, the relative magnification of the images were matched. On average, the diameter of the cornea was around 54% of the diagonal dimension of either type of image. This was achieved by using the 10 times magnification setting on the ZSL. The focal length of the PSL was adjusted to match this magnification. Second, in both image formats, the slit beam was fixed at 1.5 mm in width and angled 30° temporally from the camera axis. Third, to balance the stability disadvantage of the PSL, digital still images were extracted from video clips rather than capturing still images directly at the time of examination. Images with the correct focus and slit location could be carefully selected from a video clip. As each frame could be played slowly one by one, the effect of camera shake could be minimised. Fourth, the images were presented in similar visual angular sizes. Digital images were viewed on a

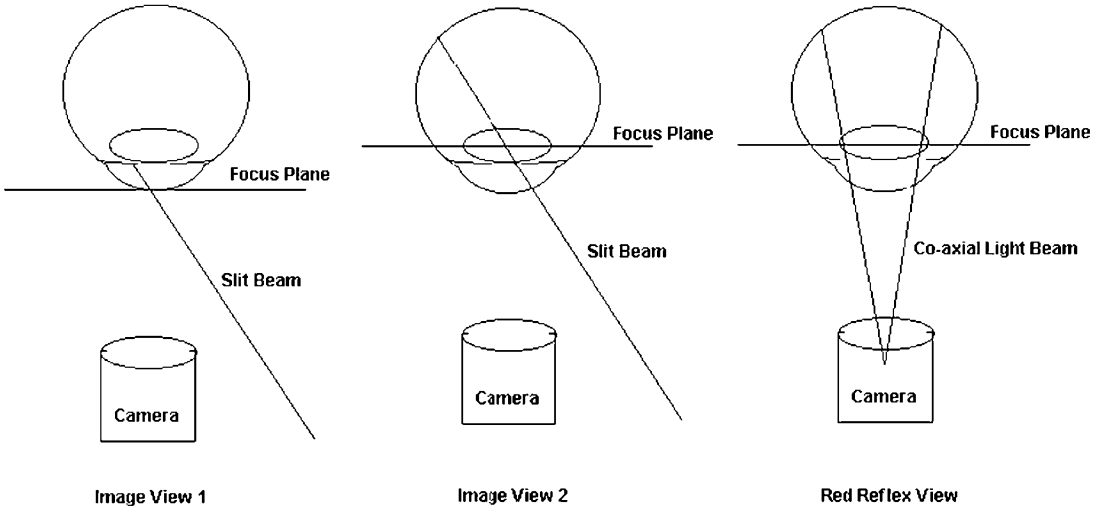

Figure 2 Diagram of portable digital slit-lamp (PSL) instrument setup. The diagram illustrates the various positions of the camera and the direction of the illumination beam as seen from above the patient for three different left eye standard views.

17-inch monitor in unchanged resolution adjusted to give a diagonal length of 15 cm and viewed at 40 cm from the screen. 35 mm slides were projected to a diagonal length of 37.5 cm and viewed at 100 cm from the screen.

Images from the PSL were compared with clinical and photographic gold standards. Traditional face-to-face ophthalmic examination by an ophthalmologist was designated as the clinical gold standard. 35 mm transparencies taken with the ZSL were designated as the photographic gold standard. Although 35 mm slit-lamp slides are not frequently used for diagnostic purposes, this imaging format is commonly used for record keeping and progress monitoring of anterior segment diseases. The comparison between the digital images and the 35 mm slides was mainly for image quality validation.

Unweighted κ statistics was used as a measure of agreement between each diagnostic modality. Sensitivity and specificity values were also calculated. The interpretation of unweighted κ statistics are as follows: 0–0.20, slight agreement; 0.21–0.40, fair agreement; 0.41–0.60, moderate agreement; 0.61–0.80, good agreement; and 0.81–1, excellent agreement. In general, most of the signs were not present in large numbers in this group of patients. The most common signs were blepharitis and cataracts. As κ statistics are grossly influenced by the prevalence of the disease,[15] these measures were not calculated in categories where there were less than 25 true positives.

Results

A total of 196 patients (392 eyes) participated in the trial. The average age of the patients was 62.5 years old (range: 15–94) and 54% of them were female. Thirty-nine patients had pupil dilation.

Table 2 summarizes the comparison between imaging modalities and the clinical findings. Digital images showed moderate to excellent agreement to clinical findings (κ 0.45–0.82) in all areas other than lid pathologies. In particular, lens signs other than posterior subcapsular opacities were well demonstrated with digital images (unweighted κ 0.54–0.75, sensitivity 76–92%, and specificity 92–99%). Gross corneal abnormalities were identified well as shown by the high sensitivity and κ values in corneal grafts (κ 0.82, sensitivity 88%, and specificity 98%), contact lens (sensitivity 67% and specificity 100%), corneal vascularisations (sensitivity 69% and specificity 99%), and corneal edemas (sensitivity 67% and specificity 99%). Small and subtle corneal signs were less well detected (for example, sensitivity of 0% for keratic precipitate and epitheliopathy). Conjunctival signs correlated moderately well with the clinical findings (κ 0.45–0.60, sensitivity 38–57%, and specificity 98–100%). Iris abnormalities were moderately well identified (sensitivity 60%). Lid pathologies were not well detected (κ 0.23 and sensitivity 0–50%). Cells and flare in the anterior chamber were not identified in the digital images (sensitivity 0%).

The results from the 35 mm transparencies were in general similar to those from the digital images. There was a wider variation in the concordance to clinical findings (κ 0.14–0.85). The trends in the statistics were similar to those found in the comparison between digital image results and clinical impressions. All the lens findings except posterior subcapsular cataracts correlated very well with the clinical gold standard (sensitivity 59–77%, specificity 86–99%, and unweighted κ 0.43–0.65). Gross corneal abnormalities were also detected well. Pterygia (κ 0.72–0.60 and sensitivity 70–54%) were better identified with 35 mm slide films. Digital images were significantly better at detection of cortical cataracts (unweighted κ 0.62 –0.43 and sensitivity 92%–59). Lid and anterior chamber signs were once again poorly detected (sensitivity 0–31%).

When the findings from the digital images were compared with those from 35 mm films, the κ, sensitivity, and specificity figures generally show the same profiles as those mentioned above. Table 3 shows the comparison between results seen in digital images and those seen in 35 mm transparencies. The two image formats generally showed more agreement to each other than to the clinical findings. κ values are 0.34–0.90 when the two image formats are compared to each other; whereas it is only 0.23–0.82 for digital images, and 0.14–0.85 for 35 mm images, when compared to clinical findings.

The assessments of the digital images from two other ophthalmologists generally showed a good agreement with the findings from the first ophthalmologist. These statistical results are shown in Table 4. Owing to the fact that only the first 100 patients were seen, the prevalence of some of the signs was very low. The statistical figures were good for the categories that showed a good agreement between the digital findings from the first ophthalmologist and clinical gold standard. For example, the agreement in lens signs other than posterior subcapsular cataracts was good to excellent (κ 0.62–0.82). There was also a good agreement in gross corneal signs like corneal grafts (sensitivity 83–60%, specificity 99–99%, and κ 0.87–0.70) and pterygia (sensitivity 53–67%, specificity 99–98%, and κ 0.62–0.67). However, in the categories that showed inadequate digital detection rates such as blepharitis, the agreement was poor (κ 0.12–0.30).

Discussion

The results from this study were limited by low prevalence in many categories of anterior segment

Table 2 35 mm film and digital images findings *vs* clinical assessment

Ocular structure	*Disease*	*N*	*TP*	*FP*	*TN*	*FN*	*Sensitivity (%)*	*Specificity (%)*	κ
Lens	Nuclear sclerosis (35 mm)	111	79[a]	24[a]	203[a]	32[a]	71	89	0.44
	Nuclear sclerosis (Digital)	109	92[a]	19[a]	203[a]	29[a]	76	91	0.54
	Cortical opacity (35 mm)	37	17[a]	12[a]	289[a]	20[a]	59	94	0.43
	Cortical opacity (Digital)	36	24[a]	12[a]	305[a]	2[a]	92	96	0.62
	Post subcapsular opacity (35 mm)	4	0[a]	1[a]	333[a]	4[a]	0	99	
	Post subcapsular opacity (Digital)	4	0[a]	4[a]	337[a]	2[a]	0	99	
	Intraocular lens (35 mm)	85	56	13	239	29	66	95	0.65
	Intraocular lens (Digital)	84	70	18	241	14	83	93	0.75
Iris	Iris abnormality (35 mm)	10	4	14	314	6	40	96	
	Iris abnormality (Digital)	10	6	11	322	4	60	97	
Anterior chamber	Cells/flare (35 mm)	5	0	0	333	5	0	100	
	Cells/flare (Digital)	5	0	0	338	5	0	100	
Cornea	Epithelial defect (35 mm)	3	1	1	334	2	33	100	
	Epithelial defect (Digital)	3	0	1	339	3	0	100	
	Oedema (35 mm)	3	2	6	329	1	67	98	
	Oedema (Digital)	3	2	3	337	1	67	99	
	Vascularisation (35 mm)	14	11	9	315	3	79	97	
	Vascularisation (Digital)	16	11	7	320	5	69	98	
	Epitheliopathy (35 mm)	16	0	0	322	16	0	100	
	Epitheliopathy (Digital)	20	0	0	323	20	0	100	
	Keratic precipitate (35 mm)	4	0	0	334	4	0	100	
	Keratic precipitate (Digital)	4	0	0	339	4	0	100	
	Scar/lipid deposit (35 mm)	14	5	4	320	9	36	99	
	Scar/lipid deposit (Digital)	17	5	4	321	13	24	98	
	Bullae (35 mm)	4	0	1	333	4	0	100	
	Bullae (Digital)	4	0	1	338	4	0	100	
	Opacification/haze (35 mm)	19	2	8	311	17	11	97	
	Opacification/haze (Digital)	17	6	7	319	11	35	98	
	Lasik flap (35 mm)	11	0	1	326	11	0	100	
	Lasik flap (Digital)	13	0	0	330	13	0	100	
	Graft (35 mm)	31	25	2	305	6	81	99	0.85
	Graft (Digital)	33	29	7	303	4	88	98	0.82
	Contact lens (35 mm)	3	3	1	334	0	100	100	
	Contact lens (Digital)	3	2	1	339	1	67	100	
Conjunctiva	Injection/conjunctivitis (35 mm)	31	6	11	296	25	19	96	0.20
	Injection/conjunctivitis (Digital)	32	12	5	306	20	38	98	0.45
	Pinguecula (35 mm)	14	4	10	314	23	29	97	
	Pinguecula (Digital)	16	7	8	319	9	44	98	
	Pterygium (35 mm)	33	23	6	299	10	70	98	0.72
	Pterygium (Digital)	30	18	6	307	12	57	98	0.60
	Haemorrhage (35 mm)	4	2	1	333	10	50	100	
	Haemorrhage (Digital)	4	2	0	339	2	50	100	
Eyelid	Trichiasis (35 mm)	6	0	2	332	6	0	99	
	Trichiasis (Digital)	6	3	1	336	3	50	100	
	Papilloma (35 mm)	3	0	4	330	3	0	99	
	Papilloma (Digital)	5	0	0	338	5	0	100	
	Blepharitis (35 mm)	112	34	40	331	78	31	82	0.14
	Blepharitis (Digital)	103	36	33	203	71	35	86	0.23

N = number of patients with the abnormality according to clinical findings.
TP = true positives; FP = false positives; TN = true negatives; FN = false negatives.
Digital = digital images; 35 mm = 35 mm slide images.
[a]Lens abnormalities were graded. Grading of 1+ and above was designated as positive for calculation of sensitivity and specificity.

Table 3 Digital images findings *vs* 35 mm film findings

Ocular structure	*Disease*	*FP*	*FN*	*TP*	*TN*	*Sensitivity (%)*	*Specificity (%)*	κ
Lens	Nuclear sclerosis	21[a]	33[a]	80[a]	195[a]	79	86	0.51
	Cortical opacity	14[a]	9[a]	15[a]	291[a]	52	97	0.48
	Post subcapsular opacity	0[a]	1[a]	1[a]	327[a]	100	100	
	Intraocular lens	22	4	61	242	94	92	0.77
Iris	Iris abnormality	4	6	13	306	68	99	
Anterior chamber	Cells/flare	0	0	0	329			
Cornea	Epithelial defect	1	2	0	326	0	100	
	Edema	2	5	3	319	38	99	
	Vascularisation	2	6	17	304	74	99	
	Epitheliopathy	0	0	0	329			
	Keratic precipitate	0	0	0	329			
	Scar/lipid deposit	6	5	3	315	38	98	
	Bullae	0	0	1	328	100	100	
	Haze/opacification	8	17	2	311	36	97	
	Lasik flap	0	1	0	328	0	100	
	Graft	6	0	29	294	100	98	0.90
	Contact lens	0	1	4	324	80	100	
Conjunctiva	Injection/conjunctivitis	11	25	6	296	44	97	
	Pinguecula	11	12	2	304	14	97	
	Pterygium	4	7	19	299	69	98	0.71
	Haemorrhage	2	3	0	324	0	99	
Eyelid	Trichiasis	4	2	0	323	0	99	
	Papilloma	0	3	0	326	0	100	
	Blepharitis	35	38	33	223	48	86	0.34

TP = true positives; FP = false positives; TN = true negatives; FN = false negatives.
[a]Lens abnormalities were graded. Grading of 1+ and above was designated as positive for calculation of sensitivity and specificity.

abnormalities in the subjects. Statistical measures of κ, sensitivity and specificity have diminished meaning when there are less than five subjects with the condition. Despite the low prevalence of some disease signs, it was clear that certain signs were much better detected than others. It was also evident that both imaging formats produce comparable diagnoses.

The similarity in the results from both image formats illustrated that portable digital slit-lamp images had similar diagnostic quality to that of 35 mm slides from a traditional slit-lamp camera when used in the same setup as used in this study. There were better statistical agreements when the findings from the two types of images were compared with each other, than when either is compared to the clinical findings. The significance of this outcome can be better appreciated when the digital resolutions of the two image formats are listed. The digital images used in this trial had 640×480 pixels or 0.3 megapixels. On the other hand, 35 mm slide typically has a 10–20 megapixel resolution when digitised. Hence, there is a 50-fold difference in resolution between the two formats. It is clear that poor detection of some subtle signs seen in this study was not due to a lack of image resolution.

It has to be noted that the PSL was designed to be a simple instrument with few configuration options. The ZSL is usually used with a variety of illumination, camera angle, and magnification options. For the sake of uniformity, these capacities were not used in this study.

Although both formats showed moderate to excellent agreement with clinical findings in lens and gross corneal signs, more subtle diseases were not detected well. In general, standardised views of still images in either format did not compare well with clinical examinations in diagnostic accuracy. Most notable was the poor detection of even gross eyelid and conjunctival disorders. This was because of the fact that both cameras, with the study setup, did not offer a full view of both lids or both sides of the sclera in one frame. Also, both instruments had a shallow depth of focus. While the corneal surfaces were focused, the lids, especially the lashes, were out of focus. At least four more views would be needed, if the lids and sclera were to be imaged adequately. There were several other reasons for the fact that these standardised still images compared poorly with clinical assessment. First, small signs that were not adjacent to the narrow slit beam (for example, posterior subcapsular cataracts and

Table 4 Digital images findings: second ophthalmologist and third ophthalmologist *vs* first ophthalmologist

Ocular structure	*Disease*	*TP*	*FP*	*TN*	*FN*	*Sensitivity (%)*	*Specificity (%)*	κ
Lens	Nuclear sclerosis (second ophthalmologist)	65[a]	11[a]	98[a]	26[a]	86	86	0.62
	Nuclear sclerosis (third ophthalmologist)	56[a]	7[a]	117[a]	20[a]	74	94	0.72
	Cortical opacity (second ophthalmologist)	12[a]	2[a]	174[a]	12[a]	79	94	0.66
	Cortical opacity (third ophthalmologist)	11[a]	2[a]	183[a]	4[a]	73	99	0.77
	Post subcapsular opacity (second ophthalmologist)	0[a]	2[a]	195[a]	3[a]	0	98	
	Post subcapsular opacity (third ophthalmologist)	0[a]	2[a]	196[a]	2[a]	0	99	
	Intraocular lens (second ophthalmologist)	36	6	149	9	80	96	0.78
	Intraocular lens (third ophthalmologist)	41	9	146	4	91	94	0.82
Iris	Iris abnormality (second ophthalmologist)	10	3	186	1	90	98	
	Iris abnormality (third ophthalmologist)	5	4	190	1	91	99	
Anterior chamber	Cells/flare (second ophthalmologist)	0	0	200	0			
	Cells/flare (third ophthalmologist)	0	0	200	0			
Cornea	Epithelial defect (second ophthalmologist)	0	4	195	1	0	98	
	Epithelial defect (third ophthalmologist)	0	2	197	1	0	99	
	Oedema (second ophthalmologist)	2	1	194	3	40	99	
	Oedema (third ophthalmologist)	2	1	194	3	40	99	
	Vascularisation (second ophthalmologist)	10	2	185	3	77	99	
	Vascularisation (third ophthalmologist)	9	3	183	5	64	98	
	Epitheliopathy (second ophthalmologist)	0	2	198	0			
	Epitheliopathy (third ophthalmologist)	0	0	200	0			
	Keratic precipitate (second ophthalmologist)	0	0	200	0			
	Keratic precipitate (third ophthalmologist)	0	1	199	0			
	Scar/lipid deposition (second ophthalmologist)	3	2	192	3	50	99	
	Scar/lipid deposition (third ophthalmologist)	2	1	193	4	33	99	
	Bullae (second ophthalmologist)	1	0	199	0	100	100	
	Bullae (third ophthalmologist)	0	0	199	1	0	100	
	Opacification/haze (second ophthalmologist)	4	7	185	4	50	96	
	Opacification/haze (third ophthalmologist)	2	8	183	7	22	96	
	Lasik flap (second ophthalmologist)	0	0	200	0			
	Lasik flap (third ophthalmologist)	0	4	196	0			
	Graft (second ophthalmologist)	20	1	175	4	83	99	0.87
	Graft (third ophthalmologist)	15	1	174	10	60	99	0.70
	Contact lens (second ophthalmologist)	1	0	198	1	50	100	
	Contact lens (third ophthalmologist)	1	0	197	2	33	100	
Conjunctiva	Injection/conjunctivitis (second ophthalmologist)	6	12	179	3	67	94	
	Injection/conjunctivitis (third ophthalmologist)	6	5	186	3	67	97	
	Pinguecula (second ophthalmologist)	4	1	192	3	57	99	
	Pinguecula (third ophthalmologist)	5	11	182	2	71	94	
	Pterygium (second ophthalmologist)	8	2	183	7	53	99	0.62
	Pterygium (third ophthalmologist)	10	4	181	5	67	98	0.67
	Haemorrhage (second ophthalmologist)	2	0	198	0	100	100	
	Haemorrhage (third ophthalmologist)	1	0	198	1	50	100	
Eyelid	Trichiasis (second ophthalmologist)	0	1	197	2	0	99	
	Trichiasis (third ophthalmologist)	0	0	198	2	0	100	
	Papilloma (second ophthalmologist)	0	0	200	0			
	Papilloma (third ophthalmologist)	0	0	200	0			
	Blepharitis (second ophthalmologist)	3	2	164	31	9	99	0.12
	Blepharitis (third ophthalmologist)	12	12	154	22	33	93	0.32

TP = true positives; FP = false positives; TN = true negatives; FN = false negatives.
[a]Lens abnormalities were graded. Grading of 1+ and above was designated as positive for calculation of sensitivity and specificity.

small corneal scars) were not detected. Second, the assessor's depth perception was reduced due to the lack of movement and stereopsis in the images. Third, flare and cells detection requires high magnification, which was not available to either image formats in this study. Fourth, certain examination manoeuvers such as

fluorescein staining or eyelid eversion was only available during clinical examination. Lastly, there was no patient history given to the image assessors.

The design of the study simulated a store and forward telemedicine environment. Store and forward telemedicine has several advantages over real-time telemedicine. A stored–forward system provides much higher image resolution, which is essential in ophthalmology. The maximum resolution in a teleconferencing video system is only 352×288 pixels. Also, it is much more time efficient for the clinicians. The time delay is acceptable for the majority of cases. Furthermore, the setup and running cost is less in a stored–forward system.

However, a store and forward system is highly dependant on the quality of the image captured by the remote operator. Although the regulated views used in this study were shown to be limited, there is still a need for a standardized method to capture anterior segment images other than for research purposes. The remote camera operators need to be taught to capture a series of controlled views as they may not have enough knowledge to decide which views to take. This is especially important in anterior segment ophthalmology telemedicine. Image capturing for stored–forward telemedicine is simpler when the target of interest is essentially single planed like the retina or skin. In these cases, the camera operator only has to be concerned with aligning the landmarks in two dimension and focus on the plane of interest. As the eye is a three-dimensional structure with an optical medium, there are many focal planes of interest during image capture. As demonstrated in this study, two to three still images captured from two focal planes are inadequate for accurate diagnosis. It is clear that many more images from different focal planes and different locations should be captured from each eye.

As part of the study, the PSL camera also captured 30–40 s of video from each of the patient's eyes. In these video clips, the slit beam scanned over the eyeball and eyelid several times in successive levels of focus. Each video consisted of 450–600 frames. Furthermore, a moving picture also gives a much better sense of depth. These clips should provide much more diagnostic information. Schiffman *et al*[16] has noted the advantage of store and forward video clips over stored–forward still images.

Despite the shortcoming of using two to three standard views, the moderate to good agreement (unweighted κ) between digital picture grading and clinical grading of lens pathology was very encouraging. The PSL images were shown to be significantly better for cortical opacity detection than images from the ZSL. This is most likely due to the advantage of having a selectable coaxial illumination built into the PSL. Detection of posterior subcapsular cataracts should improve if more image views of the lens were captured. The slit beam often missed the posterior pole of the lens and the camera was never focused on the posterior capsule of the lens. If the sensitivity for posterior subcapsular cataracts is adequate, the instrument could be used as a screening tool for cataracts

Conclusion

The image quality of the portable slit-lamp camera, for anterior segment diagnosis, has been shown to be comparable to a 35 mm slit-lamp camera when used in the setup described in this study. The study team will compare the findings from the movie clips with the clinical gold standard in the next phase of the trial.

Acknowledgements

This study was supported by Alvina King Post Doctoral Research Fellowship and G Ekamper Seeding Research Grant from the University of Western Australia. The funding sources had no role in study design, data collection, data analysis, data interpretation, or in the writing of the report or the decision to submit the paper for publication. Authors thank the participating patients from the Lions Eye Institute for their assistance in the study.

Competing interests

Dr S Kumar is part of the team who developed the PSL systems at the University of Western Australia. These systems are currently used in Western Australia on a not-for-profit basis.

References

1 Kumar S, Yogesan K, Goldschmidt L, Cuadros J. *Teleophthalmology*. Springer-Verlag: Berlin, 2006.
2 Charles BL. Internet-based eye care can lower costs and improve access. *Healthcare Financ Manage* 2000; **54**(4): 66–69.
3 Kumar S, Mei-Ling TK, Chavis F, Constable IJ, Yogesan K. Remote ophthalmology services: Cost comparison of telemedicine and alternate scenarios. *J Telemed Telecare* 2006; **12**: 19–22.
4 Kennedy C, Van Heerden A, Cook C, Murdoch I. Utilization and practical aspects of tele-ophthalmology between South Africa and the UK. *J Telemed Telecare* 2001; **7**: 20–22.
5 Blomdahl S, Maren N, Lof R. Teleophthalmology for the treatment in primary care of disorders in the anterior part of the eye. *J Telemed Telecare* 2001; **7**(Suppl 1): 25–26.
6 Kumar S, Yogesan K. Internet- based Eye Care: Vision 2020. *Lancet* 2005; **366**(9493): 1244–1245.
7 Bursell SE, Cavallerano J, Cavallerano A, Clermont AC, Birkmire-Peters D, Aiello LP *et al*. Stereo nonmydriatic digital-video color retinal imaging compared with early treatment diabetic retinopathy study seven standard field

35-mm stereo color photos for determining level of diabetic retinopathy. *Ophthalmology* 2001; **108**: 572–585.
8 Lim J, Labree L, Nichols T, Cardenas I. A comparison of digital nonmydriatic fundus imaging with standard 35-millimeter slide for diabetic retinopathy. *Ophthalmology* 2000; **107**: 866–870.
9 Cummings D, Morrissey S, Barondes M, Rogers L, Gustke S. Screening for diabetic retinopathy in rural areas: the potential of telemedicine. *J Rural Health* 2001; **17**: 25–31.
10 Marcus D, Brooks S, Ulrich L, Bassi FH, Laird M, Johnson M *et al*. Telemedicine diagnosis of eye disorder by direct ophthalmoscopy. *Ophthalmology* 1998; **105**: 1907–1914.
11 Shimmura S, Shinozaki N, Fukagawa K, Shimazaki J, Tsubota K. Real-time telemedicine in the clinical assessment of the ocular surface. *Am J Ophthalmol* 1998; **125**: 388–390.
12 Threlkeld A, Fahd T, Camp M, Johnson MH. Telemedical evaluation of ocular adnexa and anterior segment. *Am J Ophthalmol* 1999; **127**: 464–466.
13 Murdoch I, Bainbridge J, Taylor P, Smith L, Burns J, Rendall J. Postoperative evaluation of patients following ophthalmic surgery. *J Telemed Telecare* 2000; **6** (Suppl 1): 84–86.
14 Schiffman J, Tang R. Practice makes perfect: devising technical specs in teleophthalmology. *Telemed Telehealth Netw* 1997; **3**: 38–48.
15 Altman D. *Practical Statistics for Medical Research*. Chapman & Hall, 1991 Chapter 14: 394–439.
16 Schiffman J, Tang R. Technical challenges for implementation of tele-ophthalmology. *Telemed Today* 1997; **5**(6): 34–35.